Journal of Porphyrins and Phthalocyanines
J. Porphyrins Phthalocyanines 2020; A–I
DOI: 10.1142/S1088424620500182
(pp. 9

Published at https://www.worldscinet.com/jpp/

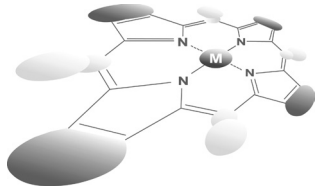

Fluorous phthalocyanines and subphthalocyanines

Kosuke Yoshinaga, Leo Delage-Laurin and Timothy M. Swager*

Department of Chemistry, Massachusetts Institute of Technology, 77 Massachusetts Ave, Cambridge, MA 02139, USA

Received 27 March 2020
Accepted 28 March 2020

ABSTRACT: Incorporating fluorine atoms into a molecule can endow it with various unique properties that enable materials applications. Selective solubility in fluorous solvents is achieved by a high fluorine content and selective partitioning into perfluorinated liquids over organic and aqueous phases provides orthogonal opportunities for chemistry and materials assembly. Although there is a growing number of partially fluorinated molecules, there are insufficient structural design principles to produce diverse fluorous soluble dyes. Herein, we report the synthesis of six fluorous phthalocyanine and subphthalocyanine dyes, and study their properties in the fluorous phase. Phthalocyanines generally display limited solubility and we also observed apparent aggregation in the fluorous phase. However, the nonplanar subphthalocyanines showed greater solubility. Subphthalocyanines also displayed fluorescence in selected solvents, and their emissive properties were investigated. The materials described expand the library of fluorous dyes and provide insights for the design of new molecules with fluorous solubility.

KEYWORDS: phthalocyanine, zinc phthalocyanine, subphthalocyanine, fluorescence, fluorine, aggregation, Faraday rotation.

INTRODUCTION

Fluorine incorporation provides properties of importance to materials chemistry and has found applications in coating materials [1], pharmaceuticals [2], *in vivo* drug delivery with perfluorocarbon nanoemulsions [3], and organic electronics [4]. Owing to fluorine's electronegativity and hydrophobicity, introducing even a single fluorine atom into a molecule can vastly influence its solubility and dipole moment [5]. As a result, there is a growing interest in incorporating fluorine into organic semiconducting materials to enhance device performance. Incorporation of fluorine has also been found to improve chemical, thermal, and photochemical stability [6]. In some cases when the incorporation of fluorine atoms is high, compounds can phase separate from organic and aqueous phases [7]. In 1994, Horváth and Rábai labeled liquids displaying this phase separation as "fluorous" phases, and demonstrated their utility in fluorous biphasic catalysis [8]. Strategies to promote fluorous phase formation and solubility therein mainly rely on the fluorine content of the molecule, and the typical requirement is that there is >50 weight percent fluorine (wt% F) [7]. However, to date examples of dyes that partition to fluorous phases over organic phases are scarce [9]. We are interested in expanding this area and have produced fluorous soluble conjugated polymers [10, 11], an array of fluorofluorophores [12], and fluorofluorescent perylene bisimides [13]. Additionally, Cao and Sletten have recently demonstrated the opportunities of fluorous character and reported the first J-aggregate in fluorous media [14] and the synthesis of a branched fluorous tag to create a fluorous soluble porphyrin [15]. All these examples give rise to noteworthy materials properties, which highlights the uniqueness of the fluorous phase. As a result, we believe many applications await the discovery with the introduction of new fluorous materials.

Fluorous phthalocyanines and subphthalocyanines have attracted our interest as a result of their applications in organic field-effect transistors [16], organic light-emitting diodes [17], photovoltaics [18], nonlinear optical materials [19], and photodynamic therapy [20]. To date there are limited reports describing the properties of phthalocyanines and subphthalocyanines in the fluorous phase [21, 22]. Herein, we report the synthesis

*Correspondence to: Timothy M. Swager, tel: +1 (617) 253-4423 email: tswager@mit.edu.

Copyright © World Scientific Publishing Company

J. Porphyrins Phthalocyanines Downloaded from www.worldscientific.com
by UPPSALA UNIVERSITY on 05/19/20. Re-use and distribution is strictly not permitted, except for Open Access articles.

J. Porphyrins Phthalocyanines Downloaded from www.worldscientific.com
by UPPSALA UNIVERSITY on 05/19/20. Re-use and distribution is strictly not permitted, except for Open Access articles.

of six fluorous soluble phthalocyanines (**F-PC**s) and subphthalocyanines (**F-SubPC**s), and elaborate on their structure–property relationship in the fluorous phase.

RESULTS AND DISCUSSION

Synthesis of F-PCs

The synthesis of **F-PC**s, as shown in Scheme 1, was accomplished by adaptation of a method previously reported in the literature [21]. In brief, phthalonitriles **1–3** were reacted with zinc acetate and 1,8-diazabicyclo[5.4.0] undec-7-ene (DBU) in *n*-pentanol to provide the desired **F-PC**s in 32–43% yields. **F-PC**s were characterized by MALDI-TOF MS, UV-vis absorbance spectroscopy, FT-IR, and elemental analysis. The low solubility of **F-PC**s in deuterated solvents and fluorous solvents prevented the acquisition of nuclear magnetic resonance (NMR) characterization.

Properties of F-PCs

The **F-PC**s displayed almost no solubility in any organic solvents, regardless of wt% F. THF was the only solvent that showed any, albeit low, solubility (<0.1 mg·mL^{-1}) of **F-PC**s. Figs 1a–1c shows the **F-PC**s partitioning into the fluorous solvent 2-(trifluoromethyl)-3-ethoxydodecafluorohexane (HFE-7500) rather than dissolving in the organic solvent diethylbenzene (DEB). The HFE-7500 and DEB solvent combination has a low interfacial tension and low upper critical mixing temperature. Although the **F-PC**s partitioned into HFE-7500, we observed precipitation of **F-PC-1** and **F-PC-2** solutions from this solvent at room temperature (Fig. S1). This was confirmed by the observation that when solutions of **F-PC-1** and **F-PC-2** were passed through a 0.2 µm syringe filter, the solution was colorless, implying that they likely form aggregates larger than 0.2 µm. The solubility of **F-PC**s can be increased to ~0.1 mg·mL^{-1} by heating the THF and HFE-7500 solutions to their boiling temperatures (66 and 128 °C, respectively). **F-PC-3** is slightly more soluble in THF and HFE-7500 than **F-PC-1** and **F-PC-2**, displaying a solubility of ~1 mg·mL^{-1}.

The photophysical properties of **F-PC**s are summarized in Table 1 and Figs 1d–1f. **F-PC-1** is scarcely soluble in heated THF and HFE-7500, and as a result its absorbance spectra were taken in THF and HFE-7500 heated to near their boiling temperatures. When solutions are cooled, the spectra broaden and decrease in intensity (Fig. S1). The heated solution was able to pass through a 0.2 µm syringe filter; however, after cooling no perceptible color was observed in filtered solutions, thereby indicating that **F-PC-1** precipitates. The absorbance spectra of **F-PC-2** and **F-PC-3** were also taken in THF and HFE-7500. The absorbance spectra of **F-PC-2** in THF resemble that reported previously [21]. The absorbance of **F-PC**s in THF showed the typical Soret and Q absorbance bands for phthalocyanines; however, a consistent large change in the spectra was observed for all of the **F-PC**s in HFE-7500. Specifically, the relative peak intensity of the Q band at ~690 nm decreased, while the relative peak intensities of the Soret band at ~360 nm, as well as the shoulder at ~650 nm increased. A decreased intensity at the $S_0 \rightarrow S_1$ band ($\lambda_{abs} \approx 690$ nm) and an increased intensity of the absorbance at ~650 nm are suggestive of H-aggregation in fluorous solvents [23, 24].

Synthesis of F-SubPCs

The synthesis of **F-SubPC**s, as shown in Scheme 2, was accomplished by adapting procedures previously reported in the literature [25]. In brief, the phthalonitrile precursors **1–3** were prepared by an S_NAr reaction of the fluoroalkyl thiols and halogenated phthalonitriles. Phthalonitriles **1–3** were then reacted with BCl_3 to provide the desired **F-SubPC**s in 13–29% yields. We note that an alternative synthetic scheme wherein the S_NAr reaction installing the fluoroalkyl thiols is performed on the halogenated subphthalocyanines did not produce the desired **F-SubPC**s (Scheme S1). The **F-SubPC**s were characterized by NMR, MALDI-TOF MS, UV-vis absorbance, fluorescence spectroscopy, FT-IR, and

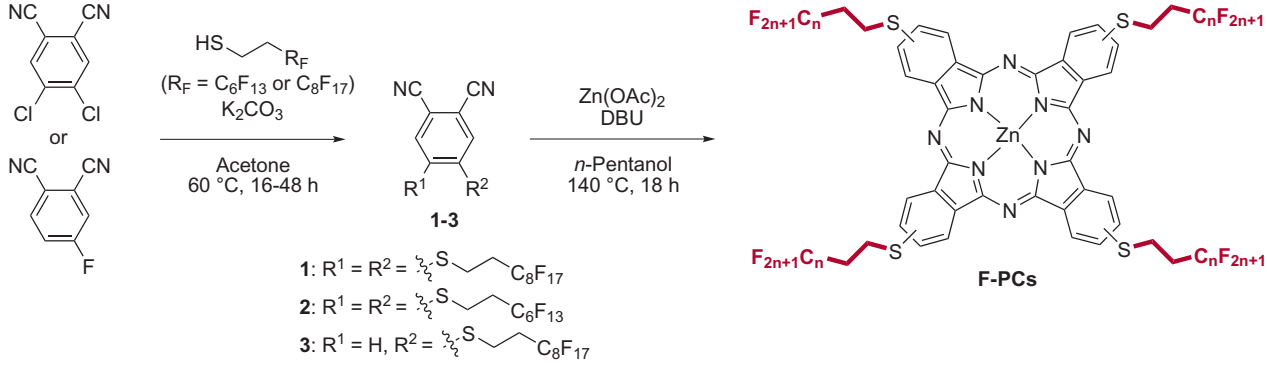

Scheme 1. Synthesis of fluorous phthalocyanines (**F-PC**s).

Copyright © World Scientific Publishing Company

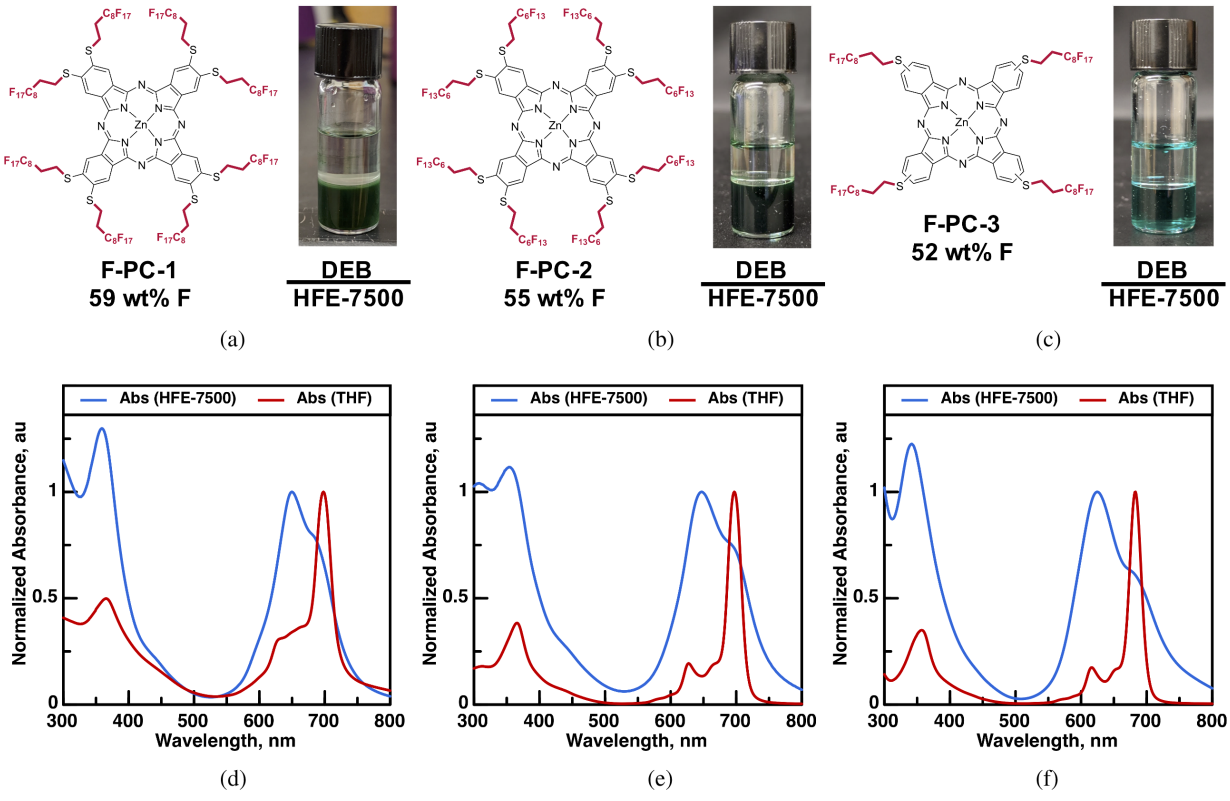

Fig. 1. Chemical structure and fluorous partition of (a) **F-PC-1**, (b) **F-PC-2**, and (c) **F-PC-3**. Overlaid normalized absorbance spectra of (d) **F-PC-1**, (e) **F-PC-2**, and (f) **F-PC-3** in organic solvent THF and in fluorous solvent HFE-7500. Spectra for **F-PC-1** obtained by heating the solutions to their boiling temperatures (66 °C for THF, 128 °C for HFE-7500).

Table 1. Summary of photophysical properties of **F-PC**s.

Compound	λ_{abs}, nm	Molar Extinction Coefficient at λ_{abs}, 10^5 L·mol^{-1}·cm^{-1})
F-PC-1	698 (THF)	1.67 (THF)
	650 (HFE-7500)	
F-PC-2	698 (THF)	2.37 (THF)
	650 (HFE-7500)	
F-PC-3	683 (THF)	2.84 (THF)
	624 (HFE-7500)	

elemental analysis. The low solubility of **F-SubPC-1** in deuterated solvents prevented the acquisition of NMR characterization.

Properties of F-SubPCs

The **F-SubPC**s are consistently more soluble than their **F-PCs** counterparts despite possessing nearly identical wt% F. **F-SubPC-1** was insoluble in common organic solvents, but was facilely soluble in fluorous solvents such as perfluoro(methylcyclohexane) (PFMCH), HFE-7500, and FC-770 (>1 mg·mL^{-1}). **F-SubPC-2** and **F-SubPC-3** displayed moderate solubility (~1 mg·mL^{-1}) in organic solvents such as chloroform and toluene (PhMe), as well as the mentioned fluorous solvents. We determined the fluorous partition coefficient (P) of **F-SubPC**s by subjecting each compound to a 1:1 mixture of PFMCH and PhMe, and quantifying the amount in each layer by UV-vis absorbance spectroscopy (Figs 2a–2c). **F-SubPC-1**, **F-SubPC-2**, and **F-SubPC-3** had a P = 36 (97:3 in PFMCH/PhMe), 1.1 (53:47 in PFMCH/PhMe), and 0.044 (4:96 in PFMCH/PhMe), respectively. From these results, we confirm a trend that higher wt% F leads to superior partitioning into fluorous solvents. The low P of **F-SubPC-3** may also be reflective of the fact that it is a regioisomeric mixture, and therefore possesses an asymmetric molecular structure.

The photophysical properties of **F-SubPC**s are summarized in Table 2 and Figs 2d–2f. In PhMe, **F-SubPC-2** and **F-SubPC-3** were fluorescent, possessing quantum yields of 25.1% and 35.2%, respectively. The limited solubility of **F-SubPC-1** in PhMe hindered the determination of the quantum yield in PhMe. The **F-SubPC**s dissolved in PFMCH also displayed a broad absorbance in the visible region, with a small hypsochromic shift. The **F-SubPC**s were only weakly fluorescent in PFMCH (Figs 2a–2c), and the quantum yields in PFMCH could not be determined.

F-SubPC-2 displayed solubility in both organic and fluorous phases to allow for comparisons, and in fluorous solvents the intensity of longest wavelength

J. Porphyrins Phthalocyanines Downloaded from www.worldscientific.com
by UPPSALA UNIVERSITY on 05/19/20. Re-use and distribution is strictly not permitted, except for Open Access articles.

Copyright © World Scientific Publishing Company

J. Porphyrins Phthalocyanines Downloaded from www.worldscientific.com
by UPPSALA UNIVERSITY on 05/19/20. Re-use and distribution is strictly not permitted, except for Open Access articles.

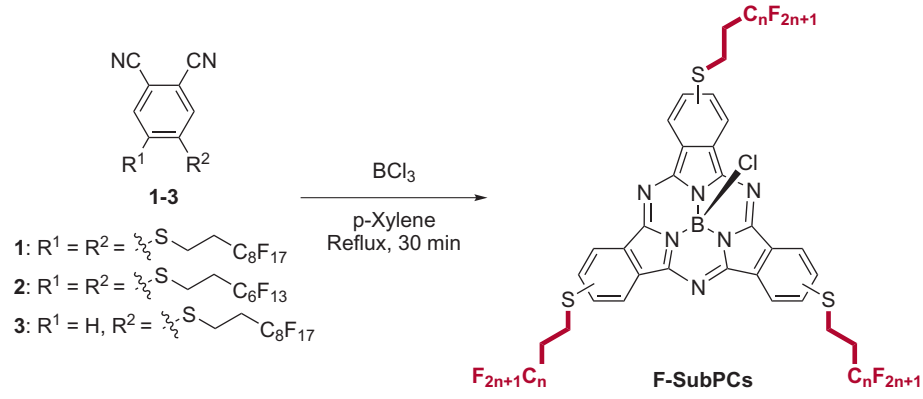

Scheme 2. Synthesis of fluorous subphthalocyanines (**F-SubPC**s).

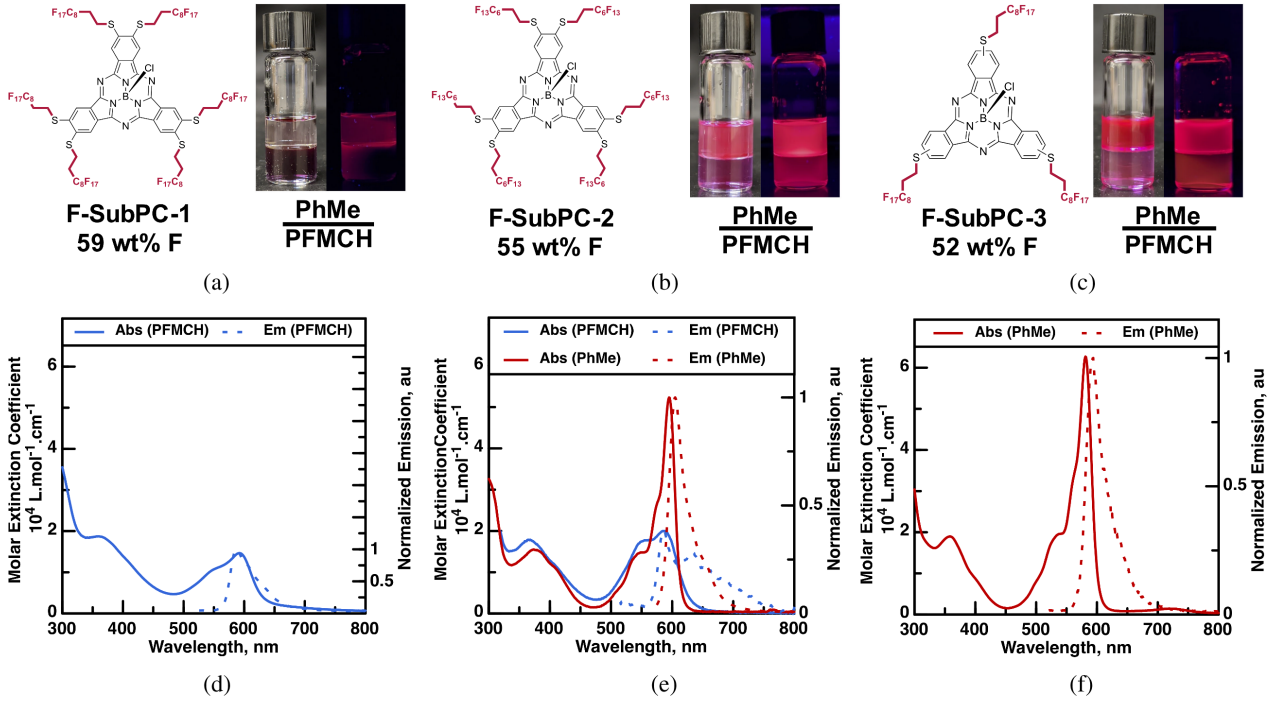

Fig. 2. Chemical structure and fluorous partition of (a) **F-SubPC-1**, (b) **F-SubPC-2**, and (c) **F-SubPC-3**. Absorbance and emission spectra of (d) **F-SubPC-1**, (e) **F-SubPC-2**, and (f) **F-SubPC-3**.

Table 2. Summary of photophysical properties of **F-SubPC**s.

Compound	Fluorous partition coefficient (PFMCH/PhMe) (*P*)	λ_{abs}, nm	Molar extinction coefficient at λ_{abs}, 10^4 L·mol^{-1}·cm^{-1})	λ_{em}, nm[a]	Quantum yield φ, %[b]	Fluorescence lifetime τ_1, ns[c]
F-SubPC-1	36	595 (PhMe)	–(PhMe)[d]	606 (PhMe)	–(PhMe)[d]	–(PhMe)[d]
		580 (PFMCH)	1.46 (PFMCH)	587 (PFMCH)	–(PFMCH)[e]	–(PFMCH)[e]
F-SubPC-2	1.1	595 (PhMe)	5.23 (PhMe)	605(PhMe)	25.1 (PhMe)	2.72 (PhMe)
		586 (PFMCH)	2.00 (PFMCH)	588 (PFMCH)	–(PFMCH)[e]	–(PFMCH)[e]
F-SubPC-3	0.044	581 (PhMe)	6.27 (PhMe)	594 (PhMe)	35.2 (PhMe)	2.87 (PhMe)
		567 (PFMCH)	–(PFMCH)[d]	573 (PFMCH)	–(PFMCH)[e]	–(PFMCH)[e]

[a]Excited at 500 nm. [b]Measured with an integrating sphere excited at 500 nm. [c]Referenced to 1,4-bis(5-phenyloxazol-2-yl)benzene (τ_1 = 1.32 ns, MeOH). [d]Not measured due to low solubility. [e]Not measured due to weak fluorescence.

Copyright © World Scientific Publishing Company

J. Porphyrins Phthalocyanines Downloaded from www.worldscientific.com
by UPPSALA UNIVERSITY on 05/19/20. Re-use and distribution is strictly not permitted, except for Open Access articles.

band (λ_{abs} ≈ 590 nm) decreased with a small increase in the absorbance at ~540 nm. This is indicative of H-aggregation in fluorous solvents, which is also likely the cause of fluorescence quenching [26]. However, the **F-SubPC**s can display fluorescence in fluorous solvents. For instance, **F-SubPC-1** is fluorescent in HFE-7500 and shows excellent partition in HFE-7500 over DEB (Fig. S2).

Faraday rotation properties of F-PCs and F-SubPCs

The Faraday effect, discovered by Michael Faraday two centuries ago, is a ubiquitous magneto-optical effect, describing the rotation of the plane-polarized light traveling through a material along the axis of an applied magnetic field [27]. This effect is quantified by a Verdet constant (**V**), which is wavelength dependent and linearly correlated to the applied magnetic field and the thickness of the material (Fig. 3). Recent emergence of organic materials possessing high Verdet constants such as semiconducting polymers [28, 29], mesogenic organic molecules [30, 31] including phthalocyanines [32, 33], and radical-containing polymers [34, 35] holds promises in utilizing these materials in processable devices. We have recently discovered that the role of polymer conformation and supramolecular organization affects the electronic delocalization and electromagnetic interactions and thereby modulates the Faraday effect [28, 34]. Because we observed H-aggregation of **F-PC**s and **F-SubPC**s in fluorous solvents, we hypothesized that the organization in fluorous solvents may give insight into the origins of the Faraday effect, and affect the degree of magnetic rotation. Thus, we sought to investigate the Faraday rotation properties of **F-PC**s and **F-SubPC**s in fluorous solvents.

Fig. 4 summarizes the Faraday rotation properties of **F-PC**s and **F-SubPC**s in various solvents (also see Fig. S4 for experimental setup). An analog property of the Verdet constant, the molar specific magnetic rotation ($deg \cdot L \cdot mol^{-1} \cdot T^{-1} \cdot m^{-1}$), was used to quantify

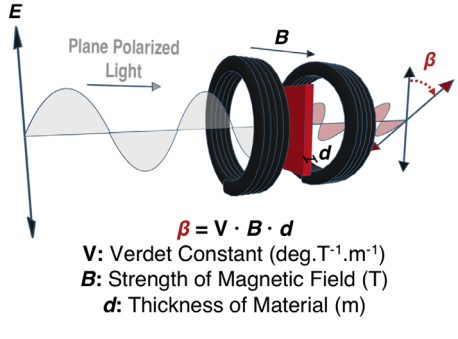

Fig. 3. Schematic image of magneto-optical material displaying a Faraday rotation. The degree of rotation (β) is governed by the materials' Verdet Constant (**V**), strength of magnetic field (***B***), and the thickness of the material (***d***).

magneto-optical effects in order to accommodate for the solution-phase nature of the samples. Because **F-PC**s displayed limited solubility in fluorous solvents, the rotation spectra could not be obtained. Instead, rotation spectra for **F-PC-2** and **F-PC-3** were obtained in THF, displaying largest molar specific magnetic rotations of -3.6×10^6 $deg \cdot L \cdot mol^{-1} \cdot T^{-1} \cdot m^{-1}$ and -8.8×10^5 $deg \cdot L \cdot mol^{-1} \cdot T^{-1} \cdot m^{-1}$, respectively. Measurement of **F-PC-2** was conducted at elevated temperatures due to its low solubility. For **F-SubPC**s, rotation spectra were obtained in fluorous solvent PFMCH for **F-SubPC-1** and **F-SubPC-2**, and in organic solvent PhMe for **F-SubPC-2** and **F-SubPC-3**. The comparison of the spectra for **F-SubPC-2** enables the study of the effect of organic and fluorous solvents on Faraday rotation properties. While we see rotation in fluorous solvent PFMCH (largest molar specific magnetic rotation of -9.3×10^4 $deg \cdot L \cdot mol^{-1} \cdot T^{-1} \cdot m^{-1}$), it is lower in intensity than that in organic solvent PhMe (largest molar specific magnetic rotation of -2.4×10^5 $deg \cdot L \cdot mol^{-1} \cdot T^{-1} \cdot m^{-1}$). Contrary to our expectations, these results confirm that H-aggregation in fluorous solvents was detrimental to the Faraday effect; however, Faraday rotation properties measured in fluorous solvents is unprecedented.

EXPERIMENTAL

General

All chemical reagents were purchased from Sigma–Aldrich, Synquest Laboratories, Oakwood Chemicals, Fluoryx Labs, or TCI, and used without purification unless noted otherwise. Thin-layer chromatography was performed with Baker-flex Silica Gel 1B-F plates (JT Baker). Flash chromatography was performed using technical grade silica gel with 60 Å pores and 230–400 mesh particle size (Sigma–Aldrich, 717185).

^{1}H, ^{13}C, and ^{19}F nuclear magnetic resonance (NMR) spectra were recorded on a JEOL model JNM-ECZ500R/S1 spectrometer operating at 500, 126, and 471 MHz, respectively. For ^{1}H and ^{13}C NMR spectra, deuterated solvent references were used as internal standards (^{1}H: 7.26 ppm for $CDCl_3$, 2.05 ppm for acetone-d_6; ^{13}C: 77.16 ppm for $CDCl_3$, 206.26 ppm for acetone-d_6). Multiplicities are abbreviated as singlet (s), doublet (d), triplet (t) and multiplet (m). Direct analysis in real time (DART) mass spectra and matrix-assisted laser desorption/ionization time-of-flight (MALDI-TOF) mass spectra were obtained at the MIT Department of Chemistry Instrumentation Facility. Elemental analysis data were obtained at Robertson Microlit Laboratories. Fourier-transform infrared spectra were obtained on a Thermo Scientific Nicolet 6700 FT-IR spectrometer. UV-vis absorbance spectra were obtained on a Cary 4000 UV-vis spectrophotometer (Agilent Technologies) with a

Copyright © World Scientific Publishing Company

J. Porphyrins Phthalocyanines Downloaded from www.worldscientific.com
by UPPSALA UNIVERSITY on 05/19/20. Re-use and distribution is strictly not permitted, except for Open Access articles.

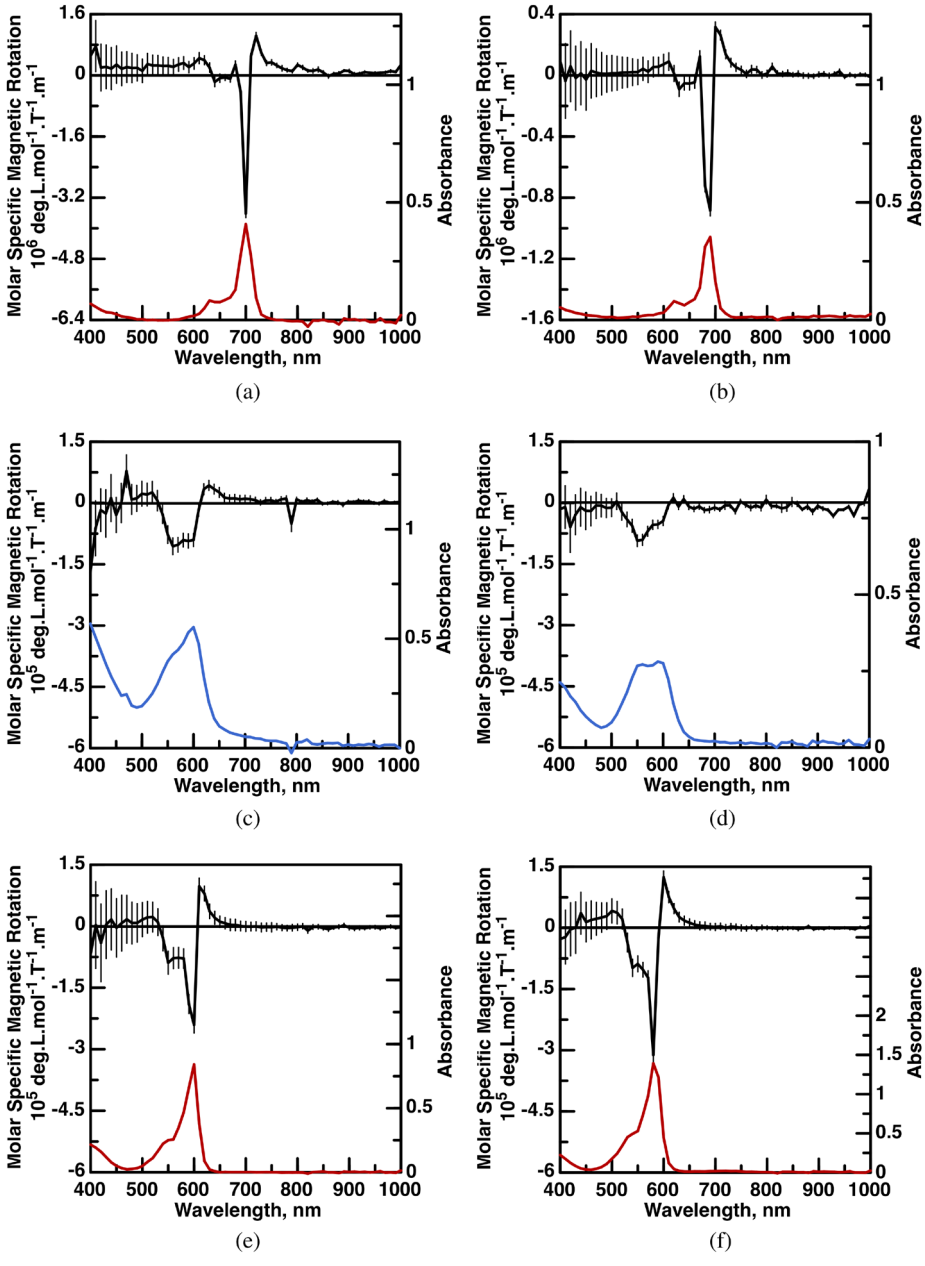

Fig. 4. Faraday rotation properties of **F-PC**s and **F-SubPC**s. Molar specific magnetic rotation of (a) **F-PC-2** and (b) **F-PC-3** in THF. Molar specific magnetic rotation of (c) **F-SubPC-1** and (d) **F-SubPC-2** in PFMCH. Molar specific magnetic rotation of (e) **F-SubPC-2** and (f) **F-SubPC-3** in PhMe. Spectra for **F-PC-2** obtained by heating the solution to its boiling temperature (66 °C).

scan rate of 600 nm.min^{-1}. The instrument was blanked on the solvent prior to obtaining a spectrum. Fluorescence spectra were obtained on a Horiba Jobin Yvon SPEX Fluorolog-τ3 fluorimeter (model FL-321, 450 W Xenon lamp). Quantum yields were determined by using Horiba Quanta–φ integrating sphere. Absorbance and fluorescence data were collected in a quartz cuvette (1 cm path length). Magneto-optical (MO) measurements were performed using our custom Faraday rotation apparatus (see Fig. S4 for experimental setup). Preparation of thin films was unsuccessful, so various solutions of **F-PC**s and **F-SubPC**s in organic and fluorous solvents were measured in a quartz cuvette (0.05 cm path length). An analog property of the Verdet constant, the molar specific magnetic rotation ($deg \cdot L \cdot mol^{-1} \cdot T^{-1} \cdot m^{-1}$), was used to quantify MO effects in order to accommodate for the solution-phase nature of the samples.

Synthesis

***Compound* 1.** A mixture of 4,5-dichlorophthalonitrile (98.5 mg, 0.500 mmol), 1*H*,1*H*,2*H*,2*H*-perfluorodecanethiol (504 mg, 1.05 mmol), and anhydrous K_2CO_3 (400 mg, 2.89 mmol) in acetone (5 mL) was stirred at

Copyright © World Scientific Publishing Company

J. Porphyrins Phthalocyanines Downloaded from www.worldscientific.com
by UPPSALA UNIVERSITY on 05/19/20. Re-use and distribution is strictly not permitted, except for Open Access articles.

60 °C for 48 h. Then, 1M HCl aq (10 mL) was added and the product precipitated. The precipitate was filtered and collected, and was recrystallized from chloroform to provide colorless crystals **1** (462 mg, 0.426 mmol, 85% yield). ^{1}H NMR (500 MHz; acetone-d_6): δ (ppm) 8.06 (s, 2H), 3.59 (t, J = 7.6 Hz, 4H), 2.68–2.84 (m, 4H). ^{13}C NMR (126 MHz; acetone-d_6): δ (ppm) 143.70, 131.54, 116.43, 113.43, 31.10 (t, J = 22 Hz), 24.35. ^{19}F NMR (471 MHz; acetone-d_6): δ (ppm) -81.56 (t, J = 9.8 Hz, 6F), -114.23 (m, 4F), -122.14 (m, 4F), -122.37 (m, 8F), -123.19 (m, 4F), -123.67 (m, 4F), -126.66 (m, 4F). DART MS: m/z calcd. for $[C_{28}H_{10}F_{34}N_2S_2]^+$: 1083.9742. Found: 1083.9742.

***Compound* 2.** Compound **2** was prepared by following a method previously reported in the literature [21]. A mixture of 4,5-dichlorophthalonitrile (197 mg, 1.00 mmol), 1*H*,1*H*,2*H*,2*H*-perfluorooctanethiol (849 mg, 2.23 mmol), and anhydrous K_2CO_3 (412 mg, 2.98 mmol) in acetone (5 mL) was stirred at 60 °C for 48 h. Then, 1M HCl aq (10 mL) was added and the product precipitated. The precipitate was filtered and collected, and was recrystallized from chloroform to provide colorless crystals **2** (789 mg, 0.892 mmol, 89% yield). ^{1}H NMR (500 MHz; acetone-d_6): δ (ppm) 8.04 (s, 2H), 3.58 (t, J = 7.6 Hz, 4H), 2.86–2.62 (m, 4H). ^{19}F NMR (471 MHz, acetone-d_6, 25°C): δ (ppm) -81.62 (t, J = 9.8 Hz, 6F), -114.26 (m, 4F), -122.39 (m, 4F), -123.39 (m, 4F), -123.74 (m, 4F), -126.73 (m, 4F). The characterization is consistent with the previous report [21].

***Compound* 3.** A mixture of 4-fluorophthalonitrile (294 mg, 2.01 mmol), 1*H*,1*H*,2*H*,2*H*-perfluorodecanethiol (985 mg, 2.05 mmol), and anhydrous K_2CO_3 (400 mg, 2.89 mmol) in acetone (5 mL) was stirred at 60 °C for 16 h. Then, 1M HCl aq (10 mL) was added and the product precipitated. The precipitate was filtered and collected, and dissolved in acetone. The acetone solution was precipitated in excess hexanes, and the precipitate was filtered and collected to provide **3** as a white solid (980 mg, 1.62 mmol, 81% yield). ^{1}H NMR (500 MHz; acetone-d_6): δ (ppm) 8.06 (s, 1H), 7.98 (d, J = 8.4 Hz, 1H), 7.88 (d, J = 8.4 Hz, 1H), 3.56 (t, J = 7.8 Hz, 2H), 2.70–2.79 (m, 2H). ^{13}C NMR (126 MHz; acetone-d_6): δ (ppm) 146.08, 134.79, 131.94, 131.85, 117.15, 116.55, 116.20, 112.42, 31.22 (t, J = 22 Hz), 23.42. ^{19}F NMR (471 MHz; acetone-d_6): δ (ppm) -81.56 (t, J = 9.8 Hz, 3F), -114.36 (m, 2F), -122.14 (m, 2F), -122.35 (m, 4F), -123.18 (m, 2F), -123.67 (m, 2F), -126.65 (m, 2F). DART MS: m/z calcd. for $C_{18}H_7F_{17}N_2S$ $[M]^+$: 606.0058. Found: 606.0071, 607.0155 $[M + H]^+$, 624.0422 $[M + NH_4]^+$, 665.0584 $[M + \text{acetone} + H]^+$.

***F-PC*-1.** A mixture of compound **1** (271 mg, 0.250 mmol), $Zn(OAc)_2$ (12.8 mg, 0.0698 mmol), and 1,8-diazabicyclo[5.4.0]undec-7-ene (DBU, 50 μL) in *n*-pentanol (5 mL) was stirred at 140 °C for 18 h. The reaction mixture was cooled to room temperature and filtered. Further purification was carried out by Soxhlet extraction with MeOH, CH_2Cl_2, and AcOEt for 24 h each to obtain **F-PC-1** as a dark green solid (114 mg, 0.0625 mmol, 41% yield). NMR and MALDI-TOF MS spectra could not be obtained due to low solubility and aggregation. Elemental Anal. calcd. for $C_{112}H_{40}F_{136}N_8S_8Zn$ (%): C, 30.55; H, 0.92; N, 2.54. Found: C, 30.53; H, 1.03; N, 3.23. UV-vis (THF): λ_{abs} (log ε) = 369 (4.9), 629 (4.7), 698 (5.2).

***F-PC*-2.** **F-PC-2** was synthesized by following a method previously reported in the literature [21]. A mixture of compound **2** (221 mg, 0.250 mmol), $Zn(OAc)_2$ (12.8 mg, 0.0698 mmol), and 1,8-diazabicyclo[5.4.0] undec-7-ene (DBU, 50 μL) in *n*-pentanol (5 mL) was stirred at 140 °C for 18 h. The reaction mixture was cooled to room temperature and filtered. Further purification was carried out by Soxhlet extraction with MeOH, CH_2Cl_2, and AcOEt for 24 h each to obtain **F-PC-2** as a green solid (97.0 mg, 0.0269 mmol, 43% yield). NMR spectra could not be obtained due to low solubility and aggregation. MALDI-TOF MS: m/z calcd. for $C_{96}H_{40}F_{104}N_8S_8Zn$ $[M]^+$: 3599.8772. Found: 3599.8692. UV-vis (THF): λ_{abs} (log ε) = 366 (5.0), 627 (4.7), 697 (5.4). The characterization is consistent with the previous literature report [21].

***F-PC*-3.** A mixture of compound **3** (152 mg, 0.251 mmol), $Zn(OAc)_2$ (12.8 mg, 0.697 mmol), and 1,8-diazabicyclo[5.4.0]undec-7-ene (DBU, 50 μL) in *n*-pentanol (5 mL) was stirred at 140 °C for 18 h. The reaction mixture was cooled to room temperature and filtered. Further purification was carried out by Soxhlet extraction with MeOH, CH_2Cl_2, and AcOEt for 24 h each to obtain **F-PC-3** as a teal-green solid (50.1 mg, 0.0201 mmol, 32% yield). NMR spectra could not be obtained due to low solubility and aggregation. MALDI-TOF MS: m/z calcd. for $C_{72}H_{28}F_{68}N_8S_4Zn$ $[M + H]^+$: 2488.9604. Found: 2488.9574. Elemental Anal. calcd. for $C_{72}H_{28}F_{68}N_8S_4Zn$ (%): C, 34.72; H, 1.13; N, 4.50. Found: C, 35.00; H, 0.56; N, 4.87. UV-vis (THF): λ_{abs} (log ε) = 357 (5.0), 616 (4.7), 683 (5.5).

***F-SubPC*-1. F-SubPC-1** was synthesized by following a method previously reported in the literature [25]. Compound **1** (462 mg, 0.426 mmol) was added to a dried flask, and BCl_3 (1.0 M in *p*-xylene, 0.450 mL) was added dropwisely. Then, the reaction mixture was stirred at 160 °C in a pre-heated oil bath for 30 min. Upon cooling the reaction mixture to room temperature, it was diluted with FC-770 (5 mL) and transferred to a separation funnel. The fluorous layer was washed with chloroform (10 mL), acetone (10 mL), water, (10 mL), brine (10 mL), dried with $MgSO_4$, and evaporated to dryness under reduced pressure. Further purification was carried out by Soxhlet extraction with acetone for 72 h to obtain **F-SubPC-1** as a dark purple solid (63.2 mg, 0.0191 mmol, 13% yield). NMR spectra could not be obtained due to low solubility and aggregation. MALDI-TOF MS: m/z calcd. for $C_{84}H_{30}BClF_{102}N_6S_6$ $[M]^+$: 3297.9009. Found: 3297.9106. UV-vis (HFE-7500): λ_{abs} (log ε) = 359 (4.3), 592 (4.2).

Copyright © World Scientific Publishing Company

J. Porphyrins Phthalocyanines Downloaded from www.worldscientific.com
by UPPSALA UNIVERSITY on 05/19/20. Re-use and distribution is strictly not permitted, except for Open Access articles.

***F-SubPC*-2.** Compound **2** (265 mg, 0.300 mmol) was added to a dried flask, and BCl_3 (1.0 M in *p*-xylene, 0.300 mL) was added dropwisely. Then, the reaction mixture was stirred at 160 °C in a pre-heated oil bath for 30 min. Upon cooling the reaction mixture to room temperature, it was diluted with FC-770 (5 mL) and transferred to a separation funnel. The fluorous layer was washed with chloroform (10 mL), acetone (10 mL), water, (10 mL), brine (10 mL), dried with $MgSO_4$, and evaporated to dryness under reduced pressure. The residue was chromatographed on silica gel using $CHCl_3$ as an eluent, and the fraction containing **F-SubPC-2** (R_f = 0.60) was collected and evaporated to dryness to provide a dark purple solid (50.2 mg, 0.0185 mmol, 19% yield). ^{1}H NMR (500 MHz; $CDCl_3$): δ (ppm) 8.76 (s, 6H), 3.38–3.49 (m, 12H), 2.49–2.64 (m, 12H). ^{19}F NMR (471 MHz; $CDCl_3$): δ (ppm) -80.79 (t, J = 9.8 Hz, 18F), -113.94 (m, 12F), -121.87 (m, 12F), -122.87 (m, 12F), -123.19 (m, 12F), -126.17 (m, 12F). MALDI-TOF MS: *m*/*z* calcd. for $C_{72}H_{30}BClF_{78}N_6S_6$ $[M + H]^+$: 2698.9471. Found: 2698.9707. Elemental Anal. calcd. for $C_{72}H_{30}BClF_{78}N_6S_6$ (%): C, 32.03; H, 1.12; N, 3.11. Found: C, 32.49; H, 1.03; N, 2.89. UV-vis (PhMe): λ_{abs} (log ε) = 373 (4.2), 595 (4.7).

***F-SubPC*-3.** Compound **3** (300 mg, 0.495 mmol) was added to a dried flask, and BCl_3 (1.0 M in *p*-xylene, 0.500 mL) was added dropwisely. Then, the reaction mixture was stirred at 160 °C in a pre-heated oil bath for 30 min. Upon cooling the reaction mixture to room temperature, it was diluted with FC-770 (5 mL) and transferred to a separation funnel. The fluorous layer was washed with chloroform (10 mL), acetone (10 mL), water, (10 mL), brine (10 mL), dried with $MgSO_4$, and evaporated to dryness under reduced pressure. The residue was chromatographed on silica gel using $CHCl_3$ as an eluent, and the fraction containing **F-SubPC-3** (R_f = 0.60) was collected and evaporated to dryness to provide a dark purple solid (90.0 mg, 0.0483 mmol, 29% yield). HPLC separation was unsuccessful. ^{1}H NMR (500 MHz; $CDCl_3$): δ (ppm) 8.76–8.83 (m, 6H), 7.85–7.89 (m, 3H), 3.35–3.48 (m, 6H), 2.48–2.59 (m, 6H). ^{19}F NMR (471 MHz; $CDCl_3$): δ (ppm) -80.78–80.51 (m, 9F), -113.60 (m, 2F), -113.99 (m, 4F), -121.59 (m, 6F), -121.82 (m, 12F), -122.62 (m, 6F), -123.15 (m, 6F), -126.01 (m, 6F). MALDI-TOF MS: *m*/*z* calcd. for $C_{54}H_{21}BClF_{51}N_6S_3$ $[M]^+$: 1863.9957. Found:1863.9942. UV-vis absorbance (PhMe): λ_{abs} (log ε) = 358 (4.3), 581 (4.8).

CONCLUSIONS

In summary, we have described the synthesis and characterization of fluorous phthalocyanines and subphthalocyanines. **F-PC-1** and **F-PC-2** displayed limited solubility in both organic and fluorous solvents, whereas **F-PC-3** was more soluble in fluorous solvents. The absorbance spectra of **F-PC**s in organic and fluorous solvents showed different trends, suggestive of H-aggregation in fluorous solvents. On the other hand, the nonplanar **F-SubPC**s showed improved solubility in fluorous solvents, and followed the trend of higher wt% F displaying higher fluorous solubility. The **F-SubPC**s were fluorescent in organic solvents and HFE-7500, but were only weakly fluorescent in PFMCH, which is also suggestive of H-aggregation. We have also studied the Faraday rotation properties of **F-PC**s and **F-SubPC**s in fluorous and organic solvents. The compounds described in this report pave the way for the discovery of functional fluorous soluble phthalocyanines and subphthalocyanines. Further characterization of the properties of **F-PC**s and **F-SubPC**s is underway, and we anticipate these compounds will find applications as new fluorous soluble/dispersible materials.

Acknowledgments

Financial support from the Air Force Office of Scientific Research (FA9550-18-1-0341) and the National Science Foundation (NSF) Center for Energy Efficient Electronics Science (E3S) (Award ECCS-0939514) is greatly appreciated. K.Y. thanks Funai Overseas Scholarship for financial support.

Supporting information

Supplementary figures and spectral data (NMR, MALDI TOF-MS) are given in the Supporting information. This material is available free of charge *via* the internet at http://worldscinet.com/jpp/jpp.shtml.

REFERENCES

1. Anton BD. *Adv. Mater.* 1998; **10**: 1197–1205.
2. Müller K, Faeh C and Diederich F. *Science*. 2007; **317**: 1881–1886.
3. Rapoport N. In *Therapeutic Ultrasound*. Escoffre J-M and Bouakaz A. (eds.) Springer International Publishing: Switzerland, 2016, pp. 221–241.
4. Ragni R, Punzi A, Babudri F and Farinola GM. *Eur. J. Org. Chem*. 2018; **2018**: 3500–3519.
5. Fuchibe K, Morikawa T, Shigeno K, Fujita T and Ichikawa J. *Org. Lett*. 2015; **17**: 1126–1129.
6. Sun H, Putta A, Kloster JP and Tottempudi UK. *Chem. Commun*. 2012; **48**: 12085–12087.
7. Horváth IT, Curran DP and Gladysz JA. In *Handbook of Fluorous Chemistry*, Gladysz JA, Curran DP and Horváth IT. John Wiley & Sons, Ltd: Hoboken, New Jersey, 2005, pp. 1–4.
8. Horváth IT and Rábai J. *Science*. 1994; **266**: 72–75.
9. Kobayashi N and Fukuda T. In *Functional Dyes*, Kim S-H (ed.) Elsevier Science: Amsterdam, 2006, pp. 1–45.
10. Lim J and Swager TM. *Angew. Chem, Int. Ed*. 2010; **49**: 7486–7488.

Copyright © World Scientific Publishing Company

11. Takeda Y, Andrew TL, Lobez JM, Mork AJ and Swager TM. *Angew. Chem, Int. Ed*. 2012; **51**: 9042–9046.
12. Sletten EM and Swager TM. *J. Am. Chem. Soc*. 2014; **136**: 13574–13577.
13. Yoshinaga K and Swager TM. *Synlett* 2018; **29**: 2509–2514.
14. Cao W and Sletten EM. *J. Am. Chem. Soc*. 2018; **140**: 2727–2730.
15. Miller MA and Sletten EM. *Org. Lett*. 2018; **20**: 6850–6854.
16. Melville OA, Lessard BH and Bender TP. *ACS Appl. Mater. Interfaces* 2015; **7**: 13105–13118.
17. Baeg K-J, Binda M, Natali D, Caironi M and Noh Y-Y. *Adv. Mater.* 2013; **25**: 4267–4295.
18. de la Torre G, Bottari G and Torres T. *Adv. Energy Mater*. 2017; **7**: 1601700.
19. Oluwole DO, Yagodin A V., Mkhize NC, Sekhosana KE, Martynov AG, Gorbunova YG, Tsivadze AY and Nyokong T. *Chem. — Eur. J.* 2017; **23**: 2820–2830.
20. Lo P-C, Rodríguez-Morgade MS, Pandey RK, Ng DKP, Torres T and Dumoulin F. *Chem. Soc. Rev*. 2020; **49**: 1041–1056 .
21. Gürol I, Gümüş G, Musluoğlu E, Arslan Y and Ahsen V. *J. Porphyrins Phthalocyanines* 2013; **17**: 555–563.
22. Mori S and Shibata N. Beilstein J. *Org. Chem*. 2017; **13**: 2273–2296.
23. Bilgiçli AT, Günsel A, Kandaz M and Özkaya AR. *Dalton Trans*. 2012; **41**: 7047–7056.
24. Bayda M, Dumoulin F, Hug GL, Koput J, Gorniak R and Wojcik A. *Dalton Trans*. 2017; **46**: 1914–1926.
25. Eder GM, Walker BR and McGrier PL. *RSC Adv*. 2017; **7**: 29271–29274.
26. Adachi K, Chayama K and Watarai H. *Soft Matter* 2005; **1**: 292–302.
27. Faraday M. *Philos. Trans. R. Soc. London* 1846; **136**: 1–20.
28. Wang P, Jeon I, Lin Z, Peeks MD, Savagatrup S, Kooi SE, Van Voorhis T and Swager TM. *J. Am. Chem. Soc*. 2018; **140**: 6501–6508.
29. Gangopadhyay P, Koeckelberghs G and Persoons A. *Chem. Mater*. 2011; **23**: 516–521.
30. Vandendriessche S, Van Cleuvenbergen S, Willot P, Hennrich G, Srebro M, Valev VK, Koeckelberghs G, Clays K, Autschbach J and Verbiest T. *Chem. Mater*. 2013; **25**: 1139–1143.
31. Vleugels R, Steverlynck J, Brullot W, Koeckelberghs G and Verbiest T. *J. Phys. Chem. C* 2019; **123**: 9382–9387.
32. Stephens PJ, Suëtaak W and Schatz PN. *J. Chem. Phys*. 1966; **44**: 4592–4602.
33. Shashoua VE. *J. Am. Chem. Soc*. 1965; **87**: 4044–4048.
34. Wang P, Lin S, Lin Z, D. Peeks M, Van Voorhis T and M. Swager T. *J. Am. Chem. Soc*. 2018; **140**: 10881–10889.
35. Lim C-K, Ju Cho M, Singh A, Li Q, Jin Kim W, Sub Jee H, L. Fillman K, H. Carpenter S, L. Neidig M, Baev A, T. Swihart M and N. Prasad P. *Nano Lett*. 2016; **16**: 5451–5455.

J. Porphyrins Phthalocyanines Downloaded from www.worldscientific.com
by UPPSALA UNIVERSITY on 05/19/20. Re-use and distribution is strictly not permitted, except for Open Access articles.

Copyright © World Scientific Publishing Company